



Improving upconversion luminescence efficiency in Er³⁺-doped NaYF₄ nanocrystals by two-color laser field

Yunhua Yao¹, Cheng Xu², Ye Zheng¹, Chengshuai Yang¹, Pei Liu¹, Jingxin Ding¹, Tianqing Jia¹, Jianrong Qiu², Shian Zhang^{1,3,*}, and Zhenrong Sun^{1,*}

¹ State Key Laboratory of Precision Spectroscopy, East China Normal University, Shanghai 200062, People's Republic of China

² State Key Laboratory of Silicon Materials, Zhejiang University, Hangzhou 310027, People's Republic of China

³ NYU-ECNU Institute of Physics at NYU Shanghai, Shanghai 200062, People's Republic of China

Received: 8 December 2015

Accepted: 19 February 2016

Published online:

29 February 2016

© Springer Science+Business Media New York 2016

ABSTRACT

Improving upconversion luminescence efficiency of lanthanide-doped nanocrystals is always a hot topic for scientists because of its very important application in photonics, photovoltaics, biological imaging, security printing, and therapeutics. Two-color laser field has shown to be a well-established strategy to further improve the upconversion luminescence efficiency. Here, we first propose a two-color laser field combining the 850 and 980 nm lasers to improve the green and red upconversion luminescence efficiency in Er³⁺-doped NaYF₄ nanocrystals. In this work, an important advantage for our strategy is that the population is directly pumped to the radiation energy level of the upconversion luminescence by a cooperation excitation process, but not the spontaneous decay from other higher energy levels, and so the higher luminescence enhancement efficiency can be obtained. These studies also provide a clear physical picture for the physical control mechanism of the upconversion luminescence efficiency improvement, which can pave a way to properly design the laser fields in the future study of upconversion luminescence generation and control.

Introduction

The upconversion luminescence is an interesting phenomenon, which is able to convert lower frequency photon to higher frequency emission, and has been found in kinds of materials, such as nonlinear optical crystals, laser dyes, and lanthanide-doped

luminescent materials. The physical mechanisms of upconversion phenomenon are different in different materials: the second harmonic generation (SHG) or sum frequency generation (SFG) is the main mechanism for the nonlinear optical crystals [1–4], and the two-photon absorption (TPA) or multi-photon absorption (MPA) is the main mechanism for the

Address correspondence to E-mails: sazhang@phy.ecnu.edu.cn; zrsun@phy.ecnu.edu.cn

laser dyes [5–9], while the energy transfer (ET) or excited state absorption (ESA) is the main mechanism for the lanthanide-doped luminescent materials besides TPA and MPA [10–12]. Most of the trivalent lanthanide ions have the unique properties with abundant energy levels, long excited state lifetime, high optical stability and low toxicity, and the intense upconversion luminescence is easy to be achieved under the continuous-wave (CW) laser excitation, so the lanthanide-doped luminescent materials have been applied in many related fields, such as laser source [13, 14], fiber optical communication [15], solar cells [16–18], high-density optical storage [19, 20], color displays [21, 22], security printing [23, 24], and biolabels [25, 26]. Especially, the lanthanide-doped nanocrystals show a great different property with the small particle size compared with normal bulk materials, and therefore has attracted more attention, in particular, the applications in biological labels and vivo imaging [27, 28]. In order to further extend the application of the lanthanide-doped nanocrystals, it is necessary to improve the upconversion luminescence efficiency. So far, many methods have been proposed, and these methods can be divided into two categories, one is changing the material properties, for example altering dopant-host combination [29, 30], adjusting the dopant concentration [31, 32], varying the nanoparticle size [33] and applying electric or magnetic field [34, 35], and the other one is controlling the excitation source, such as selecting proper wavelength [36], shaping the laser pulse [37–40], changing the repetition rate and pulse duration [41, 42], and utilizing dual-color laser field [43].

Two-color laser field excitation has shown to be an efficient way to improve the upconversion luminescence efficiency in single material. For example, Chen et al. realized the upconversion luminescence enhancement by a factor of about 3.05 in $\text{NaYF}_4:\text{Er}^{3+}$ nanoparticles with the two-wavelength excitation of 790 and 1520 nm [44], Chen et al. obtained the upconversion luminescence enhancement up to 20 times in $\text{BaCl}_2:\text{Er}^{3+}$ phosphors using the simultaneous excitation with two laser wavelengths of 808 and 980 nm [45], and our group achieved the upconversion luminescence enhancement in $\text{Er}^{3+}/\text{Yb}^{3+}$ -codoped glass by combining the 800 and 980 nm laser fields [46]. In this work, we first propose a scheme to improve the green and red upconversion luminescence efficiencies in glass ceramic containing

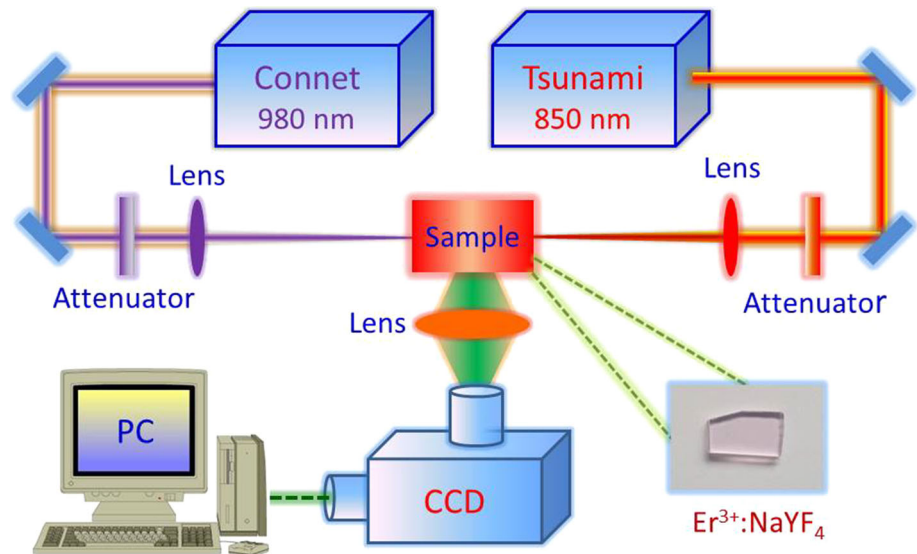
NaYF_4 nanocrystals doped with Er^{3+} ions by a two-color laser field with the laser wavelengths 850 and 980 nm. Here, the special point in our work is that almost no upconversion luminescence signal can emit when the sample is only excited by the 850 nm laser field, which is different from the previous work, where both the two laser fields can induce the intense upconversion luminescence [44–46]. We explain the physical control mechanism of the green and red upconversion luminescence enhancement under the excitation with the two-color laser field on the basis of the energy level structure of Er^{3+} ions, and also discuss the dependence of the upconversion luminescence enhancement efficiency on the two individual laser field intensities. This work is quite meaningful for the upconversion luminescence enhancement realization by the multi-color laser field excitation, where the one-color laser field cannot induce the upconversion luminescence, but can be combined to other color laser field to enhance the upconversion luminescence. In this way, the excitation source for the multi-color laser field excitation can be greatly extended, which is rather significant for the further application of lanthanide-doped luminescent materials.

Experimental arrangement

In our experiment, a fiber laser (Connet, VLSS-980-B-F-600) is used to generate the near-infrared (980 nm) continuous-wave (CW) output and a Ti-sapphire laser (Spectra-Physics, Tsunami) is used to generate the near-infrared (760–855 nm continuously tunable) CW output. The whole experimental arrangement is shown in Fig. 1, Two attenuators are, respectively, used to vary the output intensities of the two lasers, and finally the two lasers are focused into the sample in opposite direction using two lenses with the focal length of 300 mm. All luminescence signals emitted from the sample are perpendicularly collected by a lens, and measured by a spectrometer with charge-coupled device (CCD).

The sample used in our experiment is a piece of glass ceramics containing NaYF_4 nanocrystals doped with Er^{3+} ions, as shown in inset of Fig. 1. Obviously, our sample has a higher transparency, which is highly desired for further applications. The sample preparation method has been described in our previous work [39, 40], and here a simple description is

Figure 1 Schematic diagram of experimental arrangement for the upconversion luminescence enhancement in Er^{3+} -doped NaYF_4 nanocrystals by two-color laser field excitation with the Tsunami CW laser (tunable wavelength) and Connet CW laser (980 nm).



given. The precursor sample is prepared with the composition in mol. % of 40SiO_2 – $25\text{Al}_2\text{O}_3$ – $18\text{Na}_2\text{CO}_3$ – 10YF_3 – 7NaF – 1ErF_3 . The original materials are mixed and melted in a covered platinum crucible at the temperature of $1450\text{ }^\circ\text{C}$ for 45 min in the ambient atmosphere, and then are cast into a brass mold followed by annealing at the temperature of $450\text{ }^\circ\text{C}$ for 10 h. The synthesized glass is heated to the temperature of $600\text{ }^\circ\text{C}$ with an increase rate of 10 K/min , kept at this temperature for 2 h, and then cooled to room temperature to form the glass ceramic through crystallization. Finally, the sample is cut and polished for optical measurement in our experiment.

Results and discussion

The X-ray diffraction (XRD) analysis is performed to identify the crystallization phase with a power diffractometer (Bruker D8 Advance) operated at 40 kV and 40 mA, and the measurement result is shown in Fig. 2a. Here, $\text{Cu K}\alpha$ is used as radiation source, and 2θ is scanned from 10° to 80° with a step size of 0.02° . One can see that multiple sharp peaks are observed in the XRD curve, which can be attributed to cubic α - NaYF_4 crystalline phase, indicating the crystallization of α - NaYF_4 during thermal treatment. The transmission electron microscopy (TEM) is used to characterize the nanocrystal size with a field emission transmission electron microscope (JEM-2100F), and the experimental result is provided in Fig. 2b, which shows that the nanocrystals disperse

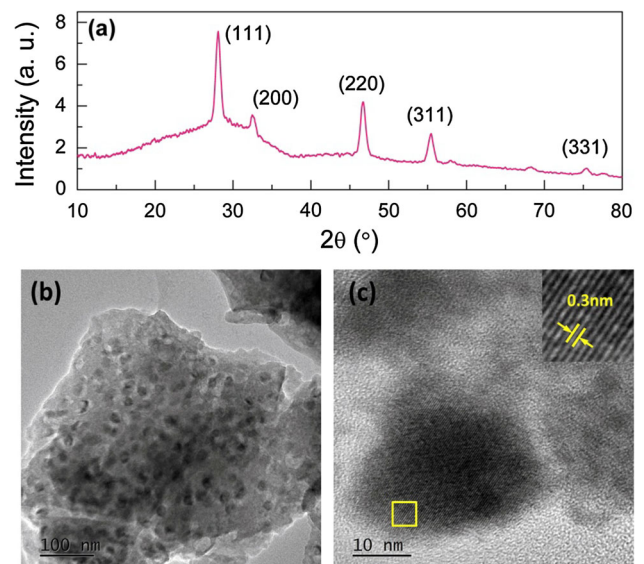


Figure 2 XRD curve (a), TEM image (b), and HRTEM image (c) of Er^{3+} -doped NaYF_4 nanocrystals.

uniformly in the glass matrix with an average size of 20–30 nm. Besides, the high-resolution TEM (HRTEM) of an individual α - NaYF_4 is further used to show the lattice fringe, as shown in Fig. 2c. It can be seen that the lattice fringe can be clearly observed, and the lattice fringe spacing is about 0.3 nm.

The absorption spectrum of the glass ceramic sample is shown in Fig. 3a, which is measured with a U-4100 spectrophotometer (HITACHI). As can be seen, ten absorption peaks are observed at 376, 415, 445, 482, 520, 560, 656, 800, 975, and 1520 nm, which

can be attributed to the transitions from the ground state $^4I_{15/2}$ to these excited states $^4G_{11/2}$, $^2H_{9/2}$, $^4F_{3/2}$, $^4F_{7/2}$, $^2H_{11/2}$, $^4S_{3/2}$, $^4F_{9/2}$, $^4I_{9/2}$, $^4I_{11/2}$, and $^4I_{13/2}$. These abundant energy levels can provide us with various two-color laser field excitation schemes to improve the upconversion luminescence efficiency.

The upconversion luminescence spectra of the glass ceramics sample excited by the 850 nm Tsunami laser field, 980 nm Connet laser field, and their combined laser field are respectively shown in Fig. 3b. For the case that the sample is only excited by the 850 nm Tsunami laser field, almost no upconversion luminescence can be observed, that is to say, the 850 nm Tsunami laser field almost cannot induce the upconversion process in the Er^{3+} -doped $NaYF_4$ nanocrystals. When the sample is only excited by the 980 nm Connet laser field, three main upconversion luminescence peaks are observed at 525, 547, and 656 nm, where the two peaks at 525 and 547 nm are called as green upconversion luminescence, which are attributed to the transitions from the two excited states $^2H_{11/2}$ and $^4S_{3/2}$ to the ground state $^4I_{15/2}$, while the peak at 656 nm is called as red upconversion luminescence, which is attributed to the transition from the excited state $^4F_{9/2}$ to the ground state $^4I_{15/2}$. However, when the glass ceramics sample is simultaneously excited by both the 850 nm Tsunami and 980 nm Connet laser fields, the spectral structure of the upconversion luminescence keeps unchanged,

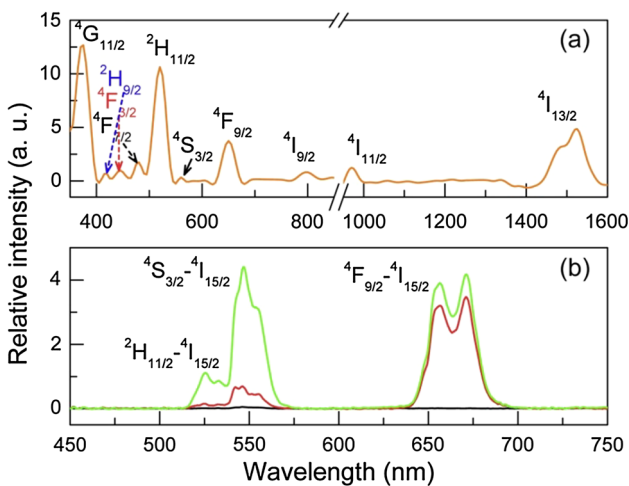


Figure 3 Absorption spectrum (a) and upconversion luminescence spectra (b) excited by 850 nm Tsunami laser field (black line), 980 nm Connet laser field (red line), and their combined laser field (green line) in Er^{3+} -doped $NaYF_4$ nanocrystals.

but compared to the sum of the luminescence intensities induced by the two individual laser field, the luminescence intensity by the combined two-field laser field is greatly enhanced. Obviously, the enhancement efficiencies for the green and red upconversion luminescence are different, and the green upconversion luminescence obtains the higher value.

To understand the physical control mechanism of the green and red upconversion luminescence efficiency improvement, we present the energy level diagram of Er^{3+} ions and possible green and red upconversion luminescence, as shown in Fig. 4. When the glass ceramics sample is excited by the 980 nm Connet laser field, the population in the ground state $^4I_{15/2}$ is pumped to the excited state $^4I_{11/2}$ by single-photon absorption, and then further pumped to the two higher excited states $^4F_{7/2}$ and $^4F_{9/2}$ by the two excited state absorption processes $^4I_{11/2} \rightarrow ^4F_{7/2}$ and $^4I_{13/2} \rightarrow ^4F_{9/2}$; here, the population in the excited state $^4I_{13/2}$ results from the spontaneous decay of the excited state $^4I_{11/2}$. The population in the excited state $^4F_{7/2}$ can spontaneously decay into the three lower excited states $^2H_{11/2}$, $^4S_{3/2}$, and $^4F_{9/2}$, and then induce the green and red upconversion luminescence. The whole excitation process is called as pathway P1. However, when the 850-nm Tsunami laser field is added to excite the glass ceramics sample, there is a cooperative excitation process in addition to the excitation process P1. The 850-nm laser wavelength is corresponding to the state transition frequency from the

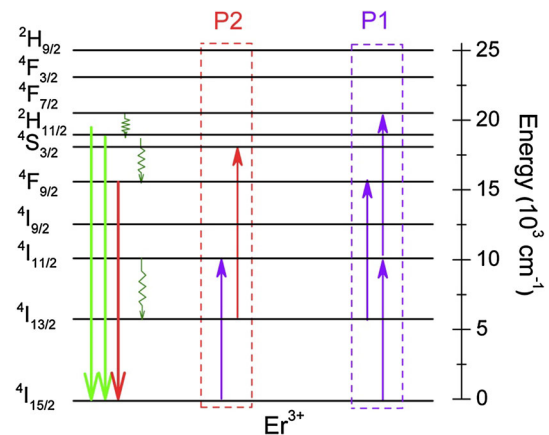


Figure 4 Energy level diagram of Er^{3+} ions and possible green and red upconversion luminescence generation by the two-color laser field with the wavelengths of 850 and 980 nm.

excited state ${}^4I_{13/2}$ to ${}^4S_{3/2}$, and thus the population in the excited state ${}^4I_{13/2}$ induced by the 980 nm Connet laser field can also be further pumped to the excited state ${}^4S_{3/2}$ by the 850-nm Tsunami laser field excitation. The population in the excited state ${}^4S_{3/2}$ will partially relax to the excited state ${}^4F_{9/2}$, and also emit the green and red upconversion luminescence. The cooperative excitation processes is called as pathway P2. Obviously, the green and red upconversion luminescence enhancement in our experiment can be attributed to the cooperative excitation process P2. Since the population in the ground state ${}^4I_{15/2}$ is directly pumped to the radiation energy level ${}^4S_{3/2}$ of the green upconversion luminescence by the cooperative excitation process P2, the green upconversion luminescence can obtain higher enhancement efficiency compared with the red upconversion luminescence.

As can be seen in Fig. 3b, the two-color laser field with the wavelengths of 850 and 980 nm is an ideal excitation source to improve the upconversion luminescence efficiency of Er^{3+} -doped NaYF_4 nanocrystals. In order to describe the improvement of the upconversion luminescence efficiency, we define the enhancement efficiency of the upconversion luminescence intensity by such a function $\eta = I_{\text{Tsu+Con}} / (I_{\text{Tsu}} + I_{\text{Con}})$, where I_{Tsu} , I_{Con} , and $I_{\text{Tsu+Con}}$ represent the upconversion luminescence intensities excited by the 850-nm Tsunami laser field, the 980-nm Connet laser field, and their combined laser field, respectively. To better understand the enhancement mechanism of the upconversion luminescence intensity, we study the dependence of the green and red upconversion luminescence intensities on the 850-nm Tsunami (or the 980-nm Connet) laser intensity. Here, we vary one laser intensity while keeping the other one at a constant. First, we measure the green and red upconversion luminescence intensities by varying the 850-nm Tsunami laser intensity, while fixing the 980-nm Connet laser intensity at 64 W/cm^2 , and the measurement results are shown in Fig. 5. In the higher 850 nm Tsunami laser intensity, a very weak green upconversion luminescence signal can be observed, which should be attributed to the weak absorption in this laser wavelength because of the proximity of 800 nm absorption bandwidth. Moreover, this weak signal almost does not affect the green upconversion luminescence enhancement efficiency. One can see that both the green and red upconversion luminescence intensities increase with

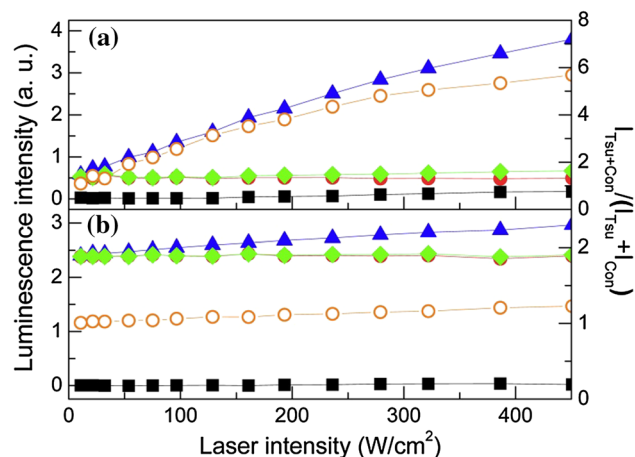


Figure 5 Left ordinate: green (a) and red (b) upconversion luminescence intensities by varying the 850-nm Tsunami laser intensity while keeping the 980-nm Connet laser intensity at 64 W/cm^2 . Black solid-square line, red solid-circle line, and blue solid-triangle line, respectively, represent the luminescence intensities induced by the 850-nm Tsunami laser field, the 980-nm Connet laser field, and their combined laser field, and green solid-rhombus line represents the sum of the luminescence intensities induced by the two individual laser fields. Right coordinate: enhancement efficiency of the luminescence intensity induced by the combined laser field with respect to the sum of that induced by the two individual laser fields $I_{\text{Tsu+Con}} / (I_{\text{Tsu}} + I_{\text{Con}})$ (orange open-circle line).

the increase of the 850-nm Tsunami laser intensity, and their enhancement efficiencies also exhibit the similar evolution behavior, but the green upconversion luminescence always obtains the higher enhancement efficiency. The phenomenon can be explained as follows. As shown in Fig. 4, using the 850-nm Tsunami laser field excitation the population in the excited state ${}^4I_{13/2}$ can be pumped to the higher excited state ${}^4S_{3/2}$, and this emits the green upconversion luminescence. However, only a fraction of population in the excited state ${}^4S_{3/2}$ can decay to the excited state ${}^4F_{9/2}$, which leads to the red upconversion luminescence. Since the cooperative excitation process P2 mainly induces the green upconversion luminescence, its enhancement efficiency will be higher. If the 850-nm Tsunami laser intensity is further increased, the enhancement efficiency will be a constant, this is because the 980-nm Connet laser intensity is invariable and therefore the population in the excited state ${}^4I_{13/2}$ is a fixed value.

Then we observe the green and red upconversion luminescence intensity evolutions by fixing the 850-nm Tsunami laser intensity at 320 W/cm^2 and

varying the 980-nm Connet laser intensity, and the experimental results are shown in Fig. 6. As can be seen, with the increase of the 980-nm Connet laser intensity, the green and red upconversion luminescence intensities also monotonously increase, but their enhancement efficiencies show first an increase followed by decrease process. The green and red upconversion luminescence intensities obtain the maximal enhancement efficiency at the 980-nm Connet laser intensity of 32 and 14 W/cm², respectively. When the 980-nm Connet laser intensity is increased, the upconversion luminescence component by the excitation process P1 will increase. Because the 850-nm Tsunami laser intensity is fixed, the transition probability from the excited states ⁴I_{13/2} to ⁴S_{3/2} will be limited. That is to say, the upconversion luminescence components by the excitation process P2 will achieve a maximal value. Thus, the weight of the excitation process P2 in the whole excitation process (P1 and P2) will decrease if the 980-nm Connet laser intensity is continuously increased, which results in the decrease of the enhancement efficiency. On the basis of the two experimental observations shown in Figs. 5 and 6, we can get a conclusion such that, to obtain the high enhancement efficiency, properly selecting the 980-nm Connet laser intensity is necessary, but the 850-nm Tsunami laser intensity can be chosen as high as possible.

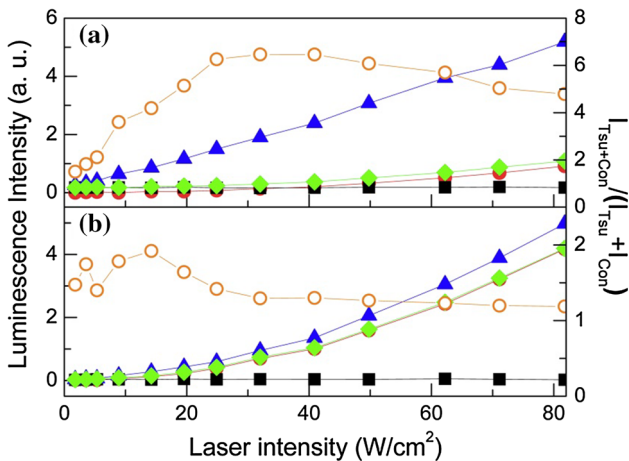


Figure 6 Green (a) and red (b) upconversion luminescence intensities by varying the 980-nm Connet laser intensity while keeping the 850-nm Tsunami laser intensity at 320 W/cm² (left coordinate), together with the enhancement efficiency of the luminescence intensity $I_{Tsu+Con}/(I_{Tsu} + I_{Con})$ (right coordinate). All the lines are labeled the same as those shown in Fig. 5.

Obviously, the two-color laser field with the wavelengths of 850 and 980 nm can provide a well-established tool to improve the green and red upconversion luminescence efficiency in Er³⁺-doped NaYF₄ nanocrystals. Compared to the red upconversion luminescence, the green upconversion luminescence can obtain much higher enhancement efficiency, and the fundamental reason is that the two-color laser field directly pumps the population to the radiation energy level ⁴S_{3/2} of the green upconversion luminescence by the cooperative excitation process P2, which is different from previous studies [44–46], where the population in the radiation energy levels comes from the spontaneous decay of the higher energy levels. The red upconversion luminescence enhancement in our experiment belongs to this case. In order to verify the advantage of our scheme, we perform the same experiment by the two-color laser field with the wavelengths of 775 and 980 nm, and the experimental results are shown in Fig. 7. Here, in addition to the laser wavelength, the other laser parameters are the same as that in Fig. 3c. Similarly, the 775-nm Tsunami laser field almost cannot induce the upconversion luminescence, but can create the excited state absorption from the excited states ⁴I_{11/2} to ⁴F_{3/2} by combining the 980-nm Connet laser field. In this case, the population in both the two radiation energy levels ⁴S_{3/2} and ⁴F_{9/2} comes from the relaxation of the higher energy level ⁴F_{3/2} by the cooperation excitation process, and thus the enhancement efficiencies of the green and red

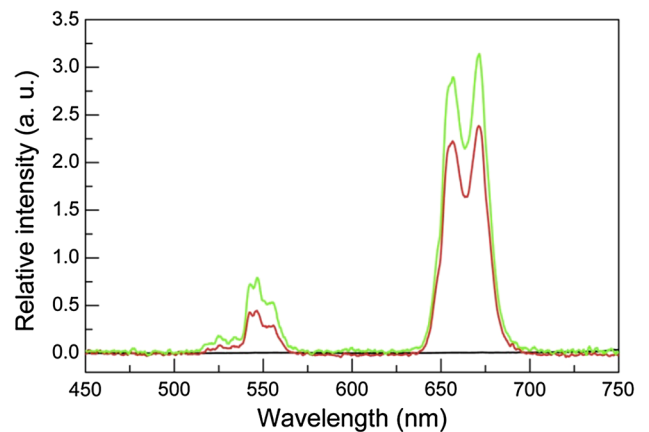


Figure 7 Upconversion luminescence spectra of Er³⁺-doped NaYF₄ nanocrystals excited by the 775-nm Tsunami laser field (black line), the 980-nm Connet laser field (red line), and their combined laser field (green line).

upconversion luminescence are both relatively low. Therefore, it is very important to choose a proper laser wavelength to pump the population to the radiation energy level by the cooperative excitation process in order to maximally improve the upconversion luminescence efficiency.

Conclusions

In this work, we have realized the green and red upconversion luminescence enhancement in glass ceramics containing NaYF_4 nanocrystals doped with Er^{3+} ions by two-color laser field with the wavelengths of 850 and 980 nm. The green upconversion luminescence can obtain the higher enhancement efficiency compared with the red upconversion luminescence, and the fundamental reason is attributed to the population being directly pumped to the radiation energy level by the cooperation excitation process. We also analyzed the dependence of the enhancement efficiency on the two individual laser field intensities, and proposed some suggestions to increase the enhancement efficiency. Furthermore, we performed the same experiment excited by the two-color laser field with the wavelengths 775 and 980 nm to further verify the advantage of our scheme in improving the upconversion luminescence efficiency. These results show that the correct choice of the laser wavelength to match the radiation energy level excitation is critical in order to obtain the high enhancement efficiency. Our work illustrated that the one-color laser field cannot induce the upconversion luminescence, but can combine other color laser field to realize the upconversion luminescence enhancement. In this sense, the excitation strategy of the upconversion luminescence generation can become more diversified, which will be of great significance for the further application of lanthanide-doped luminescent materials in various related fields.

Acknowledgements

This work was partly supported by National Natural Science Foundation of China (No. 51132004 and No. 11474096) and Science and Technology Commission of Shanghai Municipality (No. 14JC1401500). We acknowledge the support of the NYU-ECNU Institute of Physics at NYU Shanghai.

Compliance with ethical standards

Conflict of interest The authors declare that they have no conflict of interest.

References

- [1] Miller RC (1964) Optical second harmonic generation in piezoelectric crystals. *Appl Phys Lett* 5(1):17–19
- [2] Rentzepis PM, Pao YH (1964) Laser-induced optical second harmonic generation in organic crystals. *Appl Phys Lett* 5(8):156–158
- [3] Shah J, Damen TC, Deveaud B, Block D (1987) Subpicosecond luminescence spectroscopy using sum frequency generation. *Appl Phys Lett* 50(19):1307–1309
- [4] Shah J (1988) Ultrafast luminescence spectroscopy using sum frequency generation. *IEEE J Quantum Electron* 24(2):276–288
- [5] Pawlicki M, Collins HA, Denning RG, Anderson HL (2009) Two-photon absorption and the design of two-photon dyes. *Angew Chem Int Ed* 48(18):3244–3266
- [6] Denk W, Strickler JH, Webb WW (1990) Two-photon laser scanning fluorescence microscopy. *Science* 248(4951):73–76
- [7] Bhawalkar JD, He GS, Prasad PN (1996) Nonlinear multiphoton processes in organic and polymeric materials. *Rep Prog Phys* 59(9):1041
- [8] He GS, Tan L, Zheng Q, Prasad PN (2008) Multiphoton absorbing materials: molecular designs, characterizations, and applications. *Chem Rev* 108(4):1245–1330
- [9] Delysse S, Filloux P, Dumarcher V, Fiorini C, Nunzi J (1998) Multiphoton absorption in organic dye solutions. *Opt Mater* 9(1):347–351
- [10] Bloembergen N (1959) Solid state infrared quantum counters. *Phys Rev Lett* 2(3):84
- [11] Scheps R (1996) Upconversion laser processes. *Prog Quant Electron* 20(4):271–358
- [12] Wright JC (1976) Up-conversion and excited state energy transfer in rare-earth doped materials Radiationless processes in molecules and condensed phases. Springer, pp 239–295
- [13] Nilsson J, Clarkson WA, Selvas R, Sahu JK, Turner PW, Alam S, Grudinin AB (2004) High-power wavelength-tunable cladding-pumped rare-earth-doped silica fiber lasers. *Opt Fiber Technol* 10(1):5–30
- [14] Wintner E, Sorokin E, Sorokina IT (2001) Recent developments in diode-pumped ultrashort pulse solid-state lasers. *Laser Phys* 11(11):1193–1200
- [15] Zhou P, Wang X, Ma Y, Lü H, Liu Z (2012) Review on recent progress on mid-infrared fiber lasers. *Laser Phys* 22(11):1744–1751

- [16] Corma A, Atienzar P, Garcia H, Chane-Ching J (2004) Hierarchically mesostructured doped CeO₂ with potential for solar-cell use. *Nat Mater* 3(6):394–397
- [17] Trupke T, Green MA, Würfel P (2002) Improving solar cell efficiencies by up-conversion of sub-band-gap light. *J Appl Phys* 92(7):4117–4122
- [18] Wang HQ, Batentschuk M, Osvet A, Pinna L, Brabec CJ (2011) Rare-earth ion doped up-conversion materials for photovoltaic applications. *Adv Mater* 23(22–23):2675–2680
- [19] Ma D, Wu Y, Zuo X (2005) Rare earth doped β -diketone complexes as promising high-density optical recording materials for blue optoelectronics. *Mater Lett* 59(28):3678–3681
- [20] Zhang C, Zhou HP, Liao LY, Feng W, Sun W, Li ZX, Xu CH, Fang CJ, Sun LD, Zhang YW (2010) Luminescence modulation of ordered upconversion nanopatterns by a photochromic diarylethene: rewritable optical storage with nondestructive readout. *Adv Mater* 22(5):633–637
- [21] Downing E, Hesselink L, Ralston J, Macfarlane R (1996) A three-color, solid-state, three-dimensional display. *Science* 273(5279):1185–1189
- [22] Deng R, Qin F, Chen R, Huang W, Hong M, Liu X (2015) Temporal full-colour tuning through non-steady-state upconversion. *Nat Nanotechnol* 10(3):237–242
- [23] Anh TK, Loc DX, Huong TT, Vu N, Minh Le Quoc (2011) Luminescent nanomaterials containing rare earth ions for security printing. *Int J Nanotechnol* 8(3–5):335–346
- [24] Meruga JM, Cross WM, May PS, Luu Q, Crawford GA, Kellar JJ (2012) Security printing of covert quick response codes using upconverting nanoparticle inks. *Nanotechnology* 23(39):395201
- [25] Wang F, Tan WB, Zhang Y, Fan X, Wang M (2006) Luminescent nanomaterials for biological labelling. *Nanotechnology* 17(1):R1
- [26] Wolska E, Kaszewski J, Kielbik P, Grzyb J, Godlewski MM, Godlewski M (2014) Rare earth activated ZnO nanoparticles as biomarkers. *Opt Mater* 36(10):1655–1659
- [27] Kumar R, Nyk M, Ohulchanskyy TY, Flask CA, Prasad PN (2009) Combined optical and MR bioimaging using rare earth ion doped NaYF₄ nanocrystals. *Adv Funct Mater* 19(6):853–859
- [28] Zhou J, Sun Y, Du X, Xiong L, Hu H, Li F (2010) Dual-modality in vivo imaging using rare-earth nanocrystals with near-infrared to near-infrared (NIR-to-NIR) upconversion luminescence and magnetic resonance properties. *Biomaterials* 31(12):3287–3295
- [29] Antic-Fidancev E, Hölsä J, Lastusaari M, Lupei A (2001) Dopant-host relationships in rare-earth oxides and garnets doped with trivalent rare-earth ions. *Phys Rev B* 64(19):195108
- [30] Heer S, Kömpe K, Güdel HU, Haase M (2004) Highly efficient multicolour upconversion emission in transparent colloids of lanthanide-doped NaYF₄ nanocrystals. *Adv Mater* 16(23–24):2102–2105
- [31] Wang F, Liu X (2008) Upconversion multicolor fine-tuning: visible to near-infrared emission from lanthanide-doped NaYF₄ nanoparticles. *J Am Chem Soc* 130(17):5642–5643
- [32] Wang F, Xue X, Liu X (2008) Multicolor tuning of (Ln, P)-doped YVO₄ nanoparticles by single-wavelength excitation. *Angew Chem Int Edit* 47(5):906–909
- [33] Bai X, Song H, Pan G, Lei Y, Wang T, Ren X, Lu S, Dong B, Dai Q, Fan L (2007) Size-dependent upconversion luminescence in Er³⁺/Yb³⁺-codoped nanocrystalline yttria: saturation and thermal effects. *J Phys Chem C* 111(36):13611–13617
- [34] Hao J, Zhang Y, Wei X (2011) Electric-induced enhancement and modulation of upconversion photoluminescence in epitaxial BaTiO₃: Yb/Er thin films. *Angew Chem Int Ed* 50(30):6876–6880
- [35] Liu Y, Wang D, Shi J, Peng Q, Li Y (2013) Magnetic tuning of upconversion luminescence in lanthanide-doped bifunctional nanocrystals. *Angew Chem Int Ed* 52(16):4366–4369
- [36] Franzò G, Iacona F, Vinciguerra V, Priolo F (2000) Enhanced rare earth luminescence in silicon nanocrystals. *Mater Sci Eng, B* 69:335–339
- [37] Zhang S, Lu C, Jia T, Qiu J, Sun Z (2013) Coherent phase control of resonance-mediated two-photon absorption in rare-earth ions. *Appl Phys Lett* 103(19):194104
- [38] Zhang S, Xu S, Ding J, Lu C, Jia T, Qiu J, Sun Z (2014) Single and two-photon fluorescence control of Er³⁺ ions by phase-shaped femtosecond laser pulse. *Appl Phys Lett* 104(1):014101
- [39] Yao Y, Zhang S, Zhang H, Ding J, Jia T, Qiu J, Sun Z (2014) Laser polarization and phase control of up-conversion fluorescence in rare-earth ions. *Sci Rep-UK* 4:7295
- [40] Zhang S, Yao Y, Shuwu X, Liu P, Ding J, Jia T, Qiu J, Sun Z (2015) Realizing up-conversion fluorescence tuning in lanthanide-doped nanocrystals by femtosecond pulse shaping method. *Sci Rep-UK* 5:13337
- [41] Gainer CF, Joshua GS, Romanowski M. Toward the use of two-color emission control in upconverting NaYF₄: Er³⁺, Yb³⁺ nanoparticles for biomedical imaging SPIE BiOS, 2012. International Society for Optics and Photonics, p 82310I 1-8
- [42] Gainer CF, Joshua GS, De Silva CR, Romanowski M (2011) Control of green and red upconversion in NaYF₄: Yb³⁺, Er³⁺ nanoparticles by excitation modulation. *J Mater Chem* 21(46):18530–18533
- [43] Shang X, Chen P, Cheng W, Zhou K, Ma J, Feng D, Zhang S, Sun Z, Qiu J, Jia T (2014) Fine tunable red-green

- upconversion luminescence from glass ceramic containing 5% Er^{3+} : NaYF_4 nanocrystals under excitation of two near infrared femtosecond lasers. *J Appl Phys* 116(6):063101
- [44] Chen P, Yu S, Xu B, Wang J, Sang X, Liu X, Qiu J (2014) Enhanced upconversion luminescence in NaYF_4 : er nanoparticles with multi-wavelength excitation. *Mater Lett* 128:299–302
- [45] Chen Z, Zhang X, Zeng S, Liu Z, Ma Z, Dong G, Zhou S, Liu X, Qiu J (2015) Highly efficient up-conversion luminescence in BaCl_2 : Er^{3+} phosphors via simultaneous multiwavelength excitation. *Appl Phys Express* 8(3):032301
- [46] Yao Y, Xu C, Zheng Y, Yang C, Liu P, Ding J, Jia T, Qiu J, Zhang S, Sun Z (2016) Enhancing up-conversion luminescence of $\text{Er}^{3+}/\text{Yb}^{3+}$ -codoped glass by two-color laser field excitation. *RSC Adv* 6(5):3440–3445